

Irradiation of Pyrimidine in Pure H₂O Ice with High-Energy Ultraviolet Photons

Michel Nuevo,^{1,2} Yu-Jung Chen,^{3,4} Wei-Jie Hu,⁴ Jun-Ming Qiu,⁴ Shang-Ruei Wu,⁴ Hok-Sum Fung,⁵ Ching-Chi Chu,⁴ Tai-Sone Yih,⁴ Wing-Huen Ip,⁶ and C.-Y. Robert Wu³

Abstract

The detection of nucleobases, the informational subunits of DNA and RNA, in several meteorites suggests that these compounds of biological interest were formed via astrophysical, abiotic processes. This hypothesis is in agreement with recent laboratory studies of irradiation of pyrimidine in H₂O-rich ices with vacuum UV photons emitted by an H₂-discharge lamp in the 6.9–11.3 eV (110–180 nm) range at low temperature, shown to lead to the abiotic formation of several compounds including the nucleobases uracil, cytosine, and thymine. In this work, we irradiated H₂O:pyrimidine ice mixtures under astrophysically relevant conditions (14 K, $\leq 10^{-9}$ torr) with high-energy UV photons provided by a synchrotron source in three different ranges: the 0th order light (4.1–49.6 eV, 25–300 nm), the He I line (21.2 eV, 58.4 nm), and the He II line (40.8 eV, 30.4 nm). The photo-destruction of pyrimidine was monitored with IR spectroscopy, and the samples recovered at room temperature were analyzed with liquid and gas chromatographies. Uracil and its precursor 4(3*H*)-pyrimidone were found in all samples, with absolute and relative abundances varying significantly from one sample to another. These results support a scenario in which compounds of biological interest can be formed and survive in environments subjected to high-energy UV radiation fields. Key Words: Pyrimidine—Nucleobases—Interstellar ices—Cometary ices—High-energy photons—Molecular processes—Prebiotic chemistry. Astrobiology 14, 119–131.

1. Introduction

PYRIMIDINE (C₄H₄N₂) is a key molecule of prebiotic and biological interest, as it is the structural backbone of three of the nucleobases, the subunits carrying the genetic information, used in ribonucleic (RNA) and deoxyribonucleic (DNA) acids. Pyrimidine-based biological nucleobases include uracil, cytosine, and thymine, while the two other biological nucleobases adenine and guanine are based on another *N*-heterocyclic molecule, namely, purine (C₅H₄N₄). The molecular structures of all these compounds can be found elsewhere (Nuevo *et al.*, 2009).

Pyrimidine and several other small *N*-heterocycles such as purine and pyridine have been searched for in the gas phase of the interstellar medium (ISM) for a long time, though none of these compounds have been detected to date (Simon and Simon, 1973; Kuan *et al.*, 2003, 2004; Charnley

et al., 2005; Brünken *et al.*, 2006). In contrast, several purine-based and a few pyrimidine-based compounds including biological nucleobases as well as a number of their derivatives have been found in carbonaceous chondrites such as Murchison, Murray, Orgueil, and Lonewolf Nunataks 94102 (Hayatsu, 1964; Folsome *et al.*, 1971, 1973; Hayatsu *et al.*, 1975; van der Velden and Schwartz, 1977; Stoks and Schwartz, 1979, 1981; Callahan *et al.*, 2011). Isotopic analysis of these meteoritic compounds is consistent with an extraterrestrial origin (Martins *et al.*, 2008), suggesting the existence of abiotic chemical pathways for their formation in astrophysical environments.

Therefore, it is plausible that pure and substituted *N*-heterocycles are present in the solid phase, condensed on the surface of cold, icy grains in the dense ISM (Sandford *et al.*, 2004; Bernstein *et al.*, 2005), in a similar way to what is observed for polycyclic aromatic hydrocarbons (PAHs)

¹NASA Ames Research Center, Space Science Division, Moffett Field, California, USA.

²SETI Institute, Mountain View, California, USA.

³Space Sciences Center and Department of Physics and Astronomy, University of Southern California, Los Angeles, California, USA.

⁴Department of Physics, National Central University, Zhongli, Taiwan.

⁵National Synchrotron Radiation Research Center, Hsinchu, Taiwan.

⁶Graduate Institute of Astronomy, National Central University, Zhongli, Taiwan.

and polycyclic aromatic nitrogen heterocycles (PANHs) (Allamandola *et al.*, 1989; Puget and Léger, 1989; Roelfsema *et al.*, 1996). *N*-Heterocycles, PAHs, and PANHs are believed to form via similar routes, from the polymerization of small molecules such as acetylene (C₂H₂) and nitrogen-bearing species such as cyanic (HCN) and isocyanic (HNC) acids (Frenklach and Feigelson, 1989; Ricca *et al.*, 2001).

In addition, it is worth mentioning that nucleobases have been experimentally shown to form from high-energy proton bombardment (2.5–3.0 MeV) of different combinations of carbon sources (CO, CO₂, and/or CH₄) mixed with H₂O and N₂ in the gas phase at 297 K (Kobayashi and Tsuji, 1997; Yamanashi *et al.*, 2001; Miyakawa *et al.*, 2002). Although more applicable to denser, hotter environments such as planetary atmospheres, these experiments led to the formation of uracil, cytosine, thymine, and, in a few cases, guanine and adenine in measurable quantities.

More recently, laboratory experiments in which pyrimidine mixed with pure H₂O ice was irradiated with UV photons emitted by an H₂-discharge lamp at low temperature (<25 K) showed that several photo-products derived from pyrimidine can be formed, such as the nucleobase uracil and its precursor 4(3*H*)-pyrimidone (Nuevo *et al.*, 2009). These two compounds, which are the most abundant photo-products among the singly [4(3*H*)-pyrimidone] and doubly oxidized (uracil) variants of pyrimidine in laboratory samples, have been reported in Murchison, Murray, and Orgueil meteorites (Folsome *et al.*, 1971, 1973; Lawless *et al.*, 1972; Stoks and Schwartz, 1979). 4(3*H*)-Pyrimidone and uracil were also shown to be the most stable and favorable singly and doubly oxidized products of pyrimidine, respectively, from *ab initio* quantum computations, which also indicated that the presence of H₂O as a matrix is essential for the formation of products, as it plays a role of catalyst for proton abstraction (Bera *et al.*, 2010).

However, no studies about the effect of the photon energy on H₂O:pyrimidine ice mixtures have ever been performed, although icy mantles on cold grains may experience different types of UV radiation in distinct astrophysical environments, such as the diffuse ISM, dense molecular clouds, and the solar nebula. Indeed, young stars emit energetic photons up to the extreme ultraviolet (EUV) range, which covers the spectral range between 11.7 eV (106 nm) and soft X rays (*e.g.*, Wu *et al.*, 2002). Stellar EUV emission is usually due to several atomic line transitions (Judge and Pietarila, 2004; Peter *et al.*, 2006) and is believed to affect circumstellar environments including proto-planetary nebulae, even though the intensity of such EUV radiation is estimated to be 2–3 orders of magnitude lower than that of vacuum UV radiation (Rees, 1989; Meier, 1991).

The only studies of irradiation of pyrimidine with high-energy photons were conducted recently and focused on the irradiation of pure pyrimidine in the gas phase, as well as other pure compounds of astrobiological interest such as uracil, with the use of soft X rays at 150 eV (Pilling *et al.*, 2011) and 399 eV (Mendoza *et al.*, 2013) to study the photo-destruction and photo-desorption of small *N*-heterocycles. The results of these studies suggest that the irradiation of pyrimidine with soft X rays leads mainly to the photo-destruction of pyrimidine and the subsequent formation of smaller compounds rather than the conversion of pyrimidine into larger pyrimidine-based compounds.

Therefore, to assess how high-energy UV photons may affect the formation of pyrimidine-based compounds from pyrimidine in pure H₂O in the solid phase under astrophysical conditions, we performed a series of laboratory experiments of photo-irradiation of three H₂O:pyrimidine ice mixtures at 14 K with three different UV/EUV beams provided by a synchrotron light beam, as follows: (i) the 0th order beam light, covering the broad 4.1–49.6 eV (25–300 nm) range, (ii) the He I line transition (21.2 eV, 58.4 nm), and (iii) the He II line transition (40.8 eV, 30.4 nm). In all these experiments, the relative proportions between H₂O and pyrimidine were monitored to stay in the 7:1 to 10:1 range, so that ice matrix effects were dominated by H₂O.

After irradiation, each sample was allowed to warm up to room temperature naturally. Each resulting residue was analyzed with high-performance liquid chromatography (HPLC) and gas chromatography coupled with mass spectrometry (GC-MS) to search for the presence of several pyrimidine derivatives, with a focus on the nucleobase uracil and its precursor 4(3*H*)-pyrimidone as well as photo-products resulting from the photo-dissociation of pyrimidine. After measuring the photo-stability of pyrimidine in H₂O ice when irradiated with these three different UV/EUV sources, we estimated the production yields for a few identified photo-products in order to compare them with each other as well as with previous experimental studies of irradiation of similar ice mixtures with UV photons emitted by an H₂-discharge lamp. Finally, all the results obtained are discussed from an astrobiological point of view.

2. Experimental Methods

2.1. UV/EUV photo-irradiation of ices at low temperature

Experiments were carried out in an ultrahigh-vacuum (UHV) chamber built in the Department of Physics of the National Central University in Jhongli, Taiwan. This UHV chamber is evacuated by a turbo-molecular pump (KYKY FF-160/620ZE, pumping capacity: 600 L s⁻¹), which is backed up by a dry pump (Alcatel Drytel 31) and a non-evaporative getter pump (SASE GP 50), and equipped with a closed-cycle helium cryostat (CTI-M350) (Chen *et al.*, 2014). The pressure inside the UHV chamber, which is monitored by a Granville-Phillips 370 Stabil-Ion gauge, can reach down to 1 × 10⁻¹⁰ torr. The vacuum chamber also includes an oxygen-free copper cold finger with a sample holder, which is protected by a radiation shield, and can be cooled down to 14 K. CaF₂ windows (PIKE Technologies, research grade), which are transparent in the mid-IR range (5000–815 cm⁻¹), were used as substrate for these experiments. All the parts of the cold finger are connected with 99.99% pure indium to ensure a perfect thermal conductivity. Finally, a silicon diode sensor (LakeShore DT-670-SD) was used to monitor the temperature at the sample location with a 0.1 K accuracy from 14 to 400 K with the use of a LakeShore 331S temperature controller equipped with a tunable heater.

Gas mixtures were prepared in a gas line system that consisted of four stainless-steel bottles of the same volume (300 mL) and was used to determine the relative proportions between the mixture components via their partial pressures.

Pressures in the gas line are measured with an MKS Baratron 622A gauge in the 0–10 torr range with a 0.25% accuracy. The gas line is evacuated by a turbo-molecular pump (Oerlikon Leybold TurboVac 151, pumping capacity: 145 L s⁻¹) that is backed up by an oil-sealed mechanical pump (Alcatel 2012A, pumping capacity: 450 L min⁻¹) equipped with an oil trap (molecular sieve type 13X). The background pressure in the gas line is routinely lower than 1 × 10⁻⁷ torr. When not used to mix gases, the gas line is continuously baked at 120°C to avoid any organic contamination.

Samples in the UHV chamber are monitored by a mid-infrared Fourier-transform spectrometer (ABB FTLA-2000-104) equipped with a mercury-cadmium-telluride detector. For this study, IR spectra were acquired with resolutions of 1 cm⁻¹ (background spectra and final spectra of residues) and 4 cm⁻¹ (intermediate spectra during irradiation), and averaged over 512 and 128 scans, respectively. The IR beam path was built under vacuum to avoid any contamination from atmospheric CO₂ and H₂O.

The UHV chamber was directly connected to the high-flux beamline BL03A of the National Synchrotron Radiation Research Center in Hsinchu, Taiwan, which provides a range of monochromatic and white light beams. For this particular study, we used three different energy beam configurations: the 0th order beam light (4.1–49.6 eV, 25–300 nm), the He I line (21.2 eV, 58.4 nm), and the He II line (40.8 eV, 30.4 nm). The fluxes of these different beam configurations at the sample location, measured *in situ* with a calibrated 88% transmittance nickel mesh (Chen *et al.*, 2014), are given in Table 1.

Each experiment was carried out by using one beamline configuration for the irradiation of one H₂O:pyrimidine ice mixture with relative proportions ranging from 7:1 to 9:1 (Table 1). Each ice mixture was deposited on the CaF₂ window, cooled to 14 K, and simultaneously irradiated for 20 h (0th order beam experiment) or 32 h (He I and He II line experiments) with a pressure in the vacuum chamber of ~1 × 10⁻⁹ torr. Deposition rates of pyrimidine and H₂O from their respective vapors were adjusted so that their relative abundance in the ice mixtures remained in the 7:1–10:1 range. These abundance ratios between H₂O and pyrimidine were verified by IR spectroscopy by using the bands at ~3300 cm⁻¹ (H₂O) and ~1406 cm⁻¹ (pyrimidine), with integrated band strengths of 1.7 × 10⁻¹⁶ and 6.7 × 10⁻¹⁸ cm molecule⁻¹, respectively (Hudgins *et al.*, 1993; Nuevo *et al.*, 2009). In such ice mixtures, H₂O is significantly more abundant than pyrimidine to ensure that ice matrix effects are dominated by H₂O as it is observed in interstellar and circumstellar environments.

2.2. IR analysis of the samples

Before each long experiment (20 and 32 h) of simultaneous deposition of H₂O:pyrimidine ices and irradiation with UV photons, about 1000 monolayers (ML) of each starting ice mixture was deposited onto the substrate (1 ML = 10¹⁵ molecules cm⁻²; *e.g.*, Öberg *et al.*, 2007, 2009). These 1000 ML ices were subsequently irradiated by increasing intervals from 0 to 130 min for the 0th order beam and the He II line experiments and from 0 to 160 min for the He I line experiment. Infrared spectra were recorded after each irradiation interval with a 4 cm⁻¹ resolution, and the column density of pyrimidine was monitored via its IR band near 1406 cm⁻¹ by using an integrated band strength of 6.7 × 10⁻¹⁸ cm molecule⁻¹ (Hudgins *et al.*, 1993; Nuevo *et al.*, 2009, 2012).

During each long (20 and 32 h) experiment, the chemical evolution of the samples was monitored by collecting IR spectra every 4 h with a 4 cm⁻¹ resolution. Finally, IR spectra with a 1 cm⁻¹ resolution were collected for each final ice sample (after irradiation, 14 K) and for each residue at room temperature after warm-up.

2.3. HPLC and GC-MS analysis of residues at room temperature

Residues recovered at room temperature were extracted from their CaF₂ substrates with small amounts of deionized H₂O (Merck, Spectrum grade), and the extracts were kept in clean vials. Since the volumes of water used to extract the residues were not the same for each of them, the vials with the dissolved residues were then dried under vacuum overnight (15–16 h) and redissolved in 500 μL of H₂O each (Millipore Direct-Q UV 3, purified to 18.2 MΩ cm).

The resulting dissolved samples were first analyzed with HPLC. They were injected into an Agilent 1100 Series device and separated in a Phenomenex Luna 5μ Phenyl-Hexyl column (size: 250 mm × 4.60 mm, inner diameter: 5 μm), with a volume of 5 μL for each run. Separated compounds were detected by a diode-array UV detector that recorded signals simultaneously at five wavelengths (220, 245, 256, 280, and 300 nm). In this particular study, we concentrated on the chromatograms obtained at 256 nm, which provided the best signals for the peaks of pyrimidine and its oxidized derivatives. The method used (solvent gradients and pH 5 ammonium formate buffer) are described in Nuevo *et al.* (2009). Identification of the peaks in the sample chromatograms was performed by comparing both their retention times in the 256 nm chromatograms and their UV spectra with commercial standards, dissolved to 10⁻³ M in H₂O (Millipore, 18.2 MΩ cm resistivity) and injected by using the same method as the samples.

TABLE 1. SUMMARY OF THE EXPERIMENTAL PARAMETERS FOR THE THREE SAMPLES PREPARED AT THE NATIONAL SYNCHROTRON RADIATION RESEARCH CENTER

Sample	Photon energy (eV)	Photon wavelength (nm)	H ₂ O:Pyrimidine ratio	Irradiation time (h)	Photon flux (cm ⁻² s ⁻¹)
0 th order light	4.1–49.6	25–300	7:1	20	3.08 × 10 ¹⁶
He I line	21.2	58.4	9:1	32	6.46 × 10 ¹³
He II line	40.8	30.4	7:1	32	5.55 × 10 ¹³

Samples were simultaneously deposited and irradiated for either 20 h (0th order light experiment) or 32 h (He I and He II line experiments) under similar temperature and pressure conditions (~14 K, ~1.0 × 10⁻⁹ torr).

The same samples were then analyzed with GC-MS. For this, 100 μL of each sample were transferred into small pre-baked (500°C) vials and dried under vacuum in a desiccator for 2 h. Once dry, 50 μL of a 3:1:1 mixture of *N*-(*tert*-butyldimethylsilyl)-*N*-methyltrifluoroacetamide (MTBSTFA) with 1% of *tert*-butyldimethylchlorosilane (*t*BDMCS) (Restek), dimethylformamide (Pierce, silylation grade solvent), and pyrene (Sigma-Aldrich, analytical standard, 100 ng μL^{-1} dissolved in cyclohexane) were added to each residue. These mixtures were then stirred and heated to 100°C for 1 h to convert all compounds containing α -hydrogen moieties (mainly OH groups in this particular study) into their *tert*-butyldimethylsilyl (*t*BDMS) derivatives (MacKenzie *et al.*, 1987; Casal *et al.*, 2004; Schummer *et al.*, 2009).

Separation of the samples was carried out with a Thermo Trace gas chromatograph coupled with a DSQ II mass spectrometer with a splitless injection, a Restek Rxi-5ms column (length: 30 m, inner diameter: 0.25 mm, film thickness: 0.50 μm), an injector temperature of 250°C, and a helium (carrier gas; Airgas, ultrapure) flow of 1.3 mL min^{-1} . The temperature gradient used for these separations is described in detail elsewhere (Nuevo *et al.*, 2009). Masses were recorded in the 50–550 amu range, and data analysis was performed with the Xcalibur software (Thermo Finnigan). Identification of the peaks in sample chromatograms was performed by comparing both their retention times and mass spectra with the same standards as used for HPLC analysis, which were derivatized the same way as the samples.

In the samples produced in this study, we mainly searched for pyrimidine itself, 2,2'-bipyrimidine, as well as oxidized variants of pyrimidine, including 2-hydroxypyrimidine (singly oxidized), 4(3*H*)-pyrimidone (singly oxidized), pyrimidine *N*-oxide (singly oxidized), uracil (doubly oxidized), 4,6-dihydroxypyrimidine (doubly oxidized), barbituric acid (triply oxidized), and isobarbituric acid (triply oxidized). We also searched for small aliphatic compounds, including urea and the amino acids glycine, alanine, *N*-ethylglycine, and *N*-formylglycine. The purity, origin, molecular structures, molecular weights, expected retention times in the HPLC and GC-MS devices, as well as the molecular weights of the derivatized compounds for all these standards can be found elsewhere (Materese *et al.*, 2013).

3. Results

3.1. Photo-destruction of pyrimidine in H_2O ice (*IR spectroscopy*)

3.1.1. Photo-destruction half-lives of pyrimidine. Infrared spectra were recorded for the H_2O :pyrimidine ice mixtures (1000 ML) subjected to the three different UV beams (0th order beam light, He I line, and He II line). From these spectra, we derived the column densities of pyrimidine in each ice sample by integrating its IR band at $\sim 1406 \text{ cm}^{-1}$ in the spectra. The column densities obtained were then plotted as a function of the irradiation time. As a first approach, these curves could be fitted with first-order exponential decay functions of the form:

$$N(t) = N_\infty + (N_0 - N_\infty) \exp(-t/\tau) \quad (1)$$

where $N(t)$ is the column density of pyrimidine (in molecules cm^{-2}) as a function of the time t , N_0 the column

density of pyrimidine at $t=0$, N_∞ the column density of pyrimidine at $t=\infty$ (asymptotic thickness of the ice film), and τ the characteristic time (exponential decay factor). The fits of the experimental data with such first-order exponential decay functions for all three samples (0th order beam light, He I line, and He II line), which were obtained with the Fityk software¹, are shown in Fig. 1.

Half-lives ($t_{1/2}$) correspond to the time needed for half of the pyrimidine to be destroyed, that is, the time when its column density reaches a value of $N_{1/2} = (N_0 + N_\infty)/2$, and are given by $t_{1/2} = \tau \ln 2$. The half-lives obtained for pyrimidine in each experiment are summarized in Table 2. These first-order exponential decays (Eq. 1) provide general information about the photo-stability of pyrimidine when embedded in an H_2O ice matrix and subjected to UV/EUV photons of different energies.

The half-lives measured for pyrimidine for these three samples are of the same order of magnitude as that derived for an H_2O :pyrimidine=20:1 ice mixture irradiated with an H_2 -discharge lamp (38 min; Nuevo *et al.*, 2009). The shortest half-life was measured for the residue irradiated with the 0th order light (22 min), while the half-lives derived for the residues irradiated with the He I and He II lines were found to be 47 and 35 min, respectively (Table 2).

Therefore, when pyrimidine is embedded in H_2O ice and irradiated with the broad 4.1–49.6 eV 0th order beam light, its photo-destruction half-life is significantly shorter (about half) than when it is irradiated with the H_2 -discharge lamp. This indicates that the presence of high-energy ($E > 12 \text{ eV}$) photons significantly increases the destruction and/or alteration of pyrimidine and therefore decreases its photo-destruction half-life, compared with low-energy ($E < 12 \text{ eV}$) photons. However, not all high-energy photons have a similar effect on pyrimidine, since the half-life of pyrimidine in H_2O irradiated with He II photons (40.8 eV) is comparable to that measured when it is irradiated with the H_2 -discharge lamp. The longest half-life for pyrimidine in H_2O ice was measured for the He I line experiment (47 min), which suggests that He I photons (21.2 eV) are not absorbed by pyrimidine and/or H_2O molecules as efficiently as photons of other energies.

The evolution of the column density of pyrimidine for the 0th order light and He II line experiments can actually be better fitted with a more complex function of the form:

$$N(t) = N_\infty + K_1 \exp(-t/\tau_1) + K_2 \exp(-t/\tau_2) \quad (2)$$

where K_1 and K_2 are two independent pre-exponential factors and τ_1 and τ_2 two independent characteristic times (exponential decay factors). Such a function can be seen as the sum of two first-order exponential decays (Eq. 1), usually with one characteristic time (arbitrarily, τ_1) significantly shorter than the other one (τ_2), converging to a common asymptotic value N_∞ . The fits of the experimental data with the functions described by Eq. 2 for the samples irradiated with the 0th order beam light and the He II line, which were obtained with the Fityk software, are shown in Fig. 2. They clearly indicate that the photo-destruction curves of pyrimidine for these two experiments are better fitted with such

¹Available at <http://fityk.nieto.pl>.

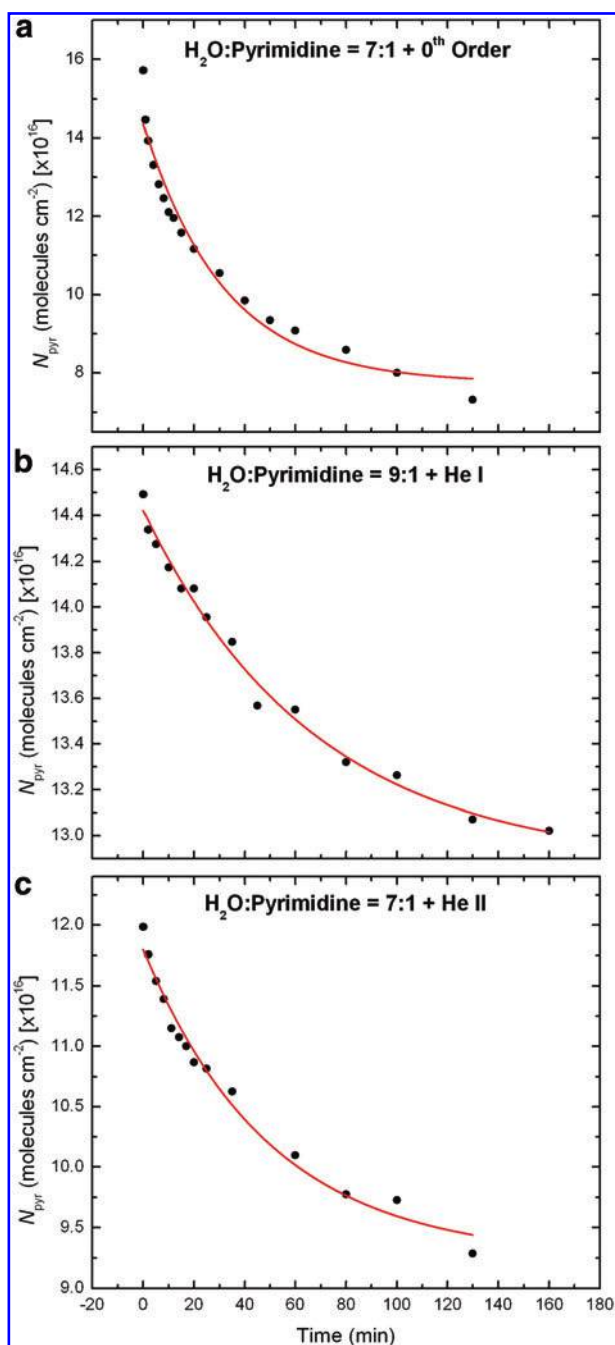


FIG. 1. Experimental data showing the decreases in column density of pyrimidine (N_{pyr}) derived from the $\sim 1406 \text{ cm}^{-1}$ bands in the IR spectra measured for the three samples irradiated with (a) the 0th order beam light, (b) the He I line, and (c) the He II line, as well as the first-order exponential decay fits of these photo-destruction curves of pyrimidine following Eq. 1. The half-lives derived from these curves are given in Table 2.

two-component exponential decay functions, with the fitting parameters summarized in Table 3. These results suggest that the photo-destruction and/or photo-conversion of pyrimidine in these two experiments take place via two distinct processes that have yet to be identified.

One possible explanation is that the photo-depletion of pyrimidine occurs via two distinct channels, one channel

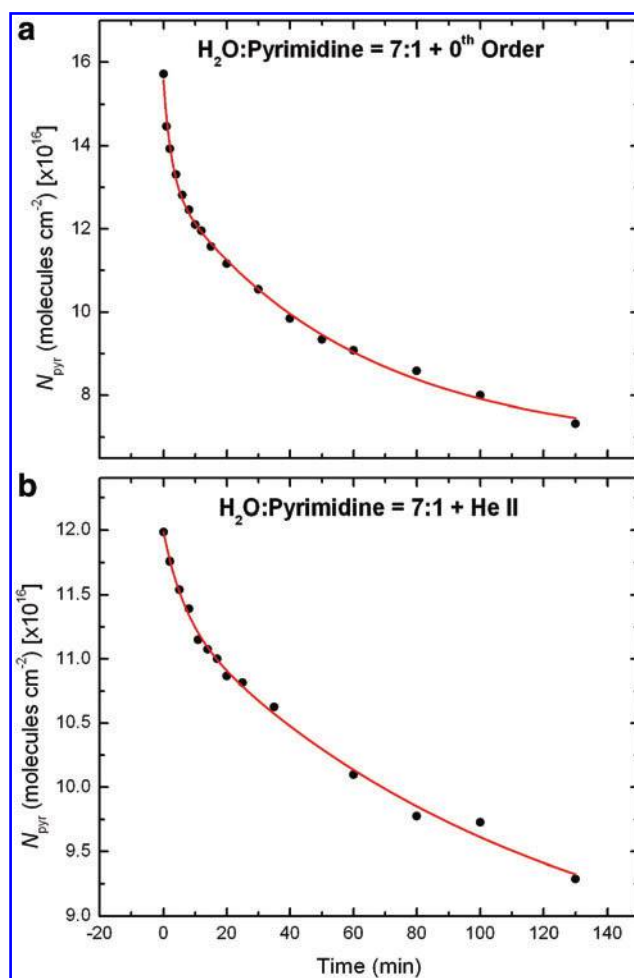


FIG. 2. Experimental data showing the decreases in column density of pyrimidine (N_{pyr}) derived from the $\sim 1406 \text{ cm}^{-1}$ bands in the IR spectra measured for the samples irradiated with (a) the 0th order beam light and (b) the He II line, as well as the two-component first-order exponential decay fits of these photo-destruction curves of pyrimidine following Eq. 2. The resulting fitting parameters for these curves are given in Table 3.

TABLE 2. COMPARISON BETWEEN THE UV/EUV PHOTO-INDUCED HALF-LIVES OF PYRIMIDINE IN PURE H₂O ICE WHEN SUBJECTED TO THE 0TH ORDER LIGHT, THE HE I LINE, AND THE HE II LINE

Experiment/UV source	Photon energy (eV)	Half-lives (min)
Synchrotron 0 th order light	4.1–49.6	22
Synchrotron He I line	21.2	47
Synchrotron He II line	40.8	35
H ₂ -discharge lamp ^a	6.9–11.3	38
Pyrimidine in argon (1:750) with H ₂ -discharge lamp ^b	6.9–11.3	0.93

These half-lives are compared with that of an H₂O:pyrimidine=20:1 ice mixture irradiated with an H₂-discharge UV lamp (Nuevo *et al.*, 2009) and with that of pyrimidine in an argon matrix (Peeters *et al.*, 2005) with a similar H₂-discharge lamp.

^aData from Nuevo *et al.* (2009).

^bData from Peeters *et al.* (2005).

TABLE 3. EXPONENTIAL PARAMETERS (N_∞ , K_1 , τ_1 , K_2 , AND τ_2) OBTAINED FOR THE BEST FITS OF THE PYRIMIDINE PHOTO-DESTRUCTION CURVES WITH THE TWO-COMPONENT EXPONENTIAL FUNCTION GIVEN IN EQ. 2 FOR THE H₂O:PYRIMIDINE ICE SAMPLES IRRADIATED WITH THE 0TH ORDER BEAM LIGHT AND THE He II LINE

Exponential parameters from Eq. 2	H ₂ O:Pyrimidine ice samples	
	0 th order	He II
N_∞ (molecules cm ⁻²)	6.88×10^{16}	8.36×10^{16}
K_1 (molecules cm ⁻²)	2.52×10^{16}	0.63×10^{16}
τ_1 (min)	2.62	6.54
K_2 (molecules cm ⁻²)	6.29×10^{16}	3.00×10^{16}
τ_2 (min)	58.79	114.30

being much slower than the other one. Irradiations with the 0th order light, the He I line, and the He II line can, in theory, all dissociate H₂O into OH radicals together with O and H atoms, as well as their respective ionized forms, since the ionization energy of both H and O is about 13.6 eV (Itikawa *et al.*, 1989). All these species would therefore become available in the ice to react with pyrimidine in its neutral, radical, and/or cationic forms (Bera *et al.*, 2010) and open new pathways for the photo-destruction and photo-conversion of pyrimidine.

However, in the case of the irradiation with the He I line (58.4 nm, 21.2 eV), the contribution of O, H, and OH ions is expected to be significantly weaker than in the 0th order and the He II experiments, because the photo-ionization cross sections for O, H, and OH at 58.4 nm are much smaller than at 30.4 nm (Stephens and McKoy, 1987; Itikawa *et al.*, 1989). This may explain why the photo-destruction curve of pyrimidine in this experiment follows a one-component first-order exponential decay (Eq. 1 and Fig. 1). In contrast, the presence of higher-energy photons in the 0th order and He II experiments will increase the population of ionized species susceptible to react with pyrimidine. The presence of these species in the ice will increase the number of reaction pathways for the photo-depletion of pyrimidine, in particular those involving O⁺, H⁺, and OH⁺, as supported by the two-component exponential decay fits for the photo-destruction of pyrimidine in these two experiments (Eq. 2 and Fig. 2). However, because of the small abundances of these ions compared with other species present in the ices, these pathways are expected to provide significantly smaller conversion yields for pyrimidine. This is in agreement with the fact that, in the two-component exponential decays describing the half-lives of pyrimidine in the 0th order and He II experiments, one of the characteristic times is always significantly longer than the other one (Table 3) and may correspond to pathways involving less abundant species such as O⁺, H⁺, and OH⁺. It is also interesting to note that the characteristic times τ_1 and τ_2 derived for the 0th order light experiments are about twice as short as those derived for the He II experiment, which is consistent with the half-lives measured for these two experiments from the one-component exponential decays (Table 2).

These results may also explain the one-component exponential decay measured for pyrimidine when it is mixed in

pure H₂O ice and subjected to the UV radiation emitted by a regular H₂-discharge lamp (Nuevo *et al.*, 2009; Table 2). Indeed, such a light source cannot ionize O, H, or OH, as the experimental ionization energy of OH was measured to be 13.017 eV (Barr *et al.*, 1999; Ruscic *et al.*, 2002). Consequently, the photo-conversion rate of pyrimidine reacting with O⁺, H⁺, and OH⁺ is expected to be much lower than that of pyrimidine directly photo-destroyed, so that such a pathway can be considered as negligible in experiments in which H₂O:pyrimidine ices are irradiated with an H₂-discharge lamp.

As a final remark, all the half-lives measured for pyrimidine in the present study are much longer than that measured for pyrimidine in an argon matrix (Table 2), which is assumed to simulate pyrimidine in the gas phase (Peeters *et al.*, 2005). This indicates that when embedded in an H₂O ice matrix, pyrimidine is always significantly more stable to UV/EUV radiation than in the gas phase, regardless of the light source employed. Extrapolating the half-lives found in our laboratory experiments to different astrophysical environments similarly to what was done previously for an H₂O:pyrimidine = 20:1 ice mixture (Nuevo *et al.*, 2009) and for pyrimidine in argon (Peeters *et al.*, 2005) irradiated with an H₂-discharge lamp is difficult here, mainly because the light sources employed in the present study have very different energy ranges. Indeed, the 0th order beam light provides photons with energies in the very broad 4.1–49.6 eV range, while the He I and He II lines are both monochromatic and thus very narrow.

Nonetheless, EUV radiation is present in astrophysical environments and more particularly in the Solar System (Judge and Pietarila, 2004; Peter *et al.*, 2006), so that pyrimidine in H₂O-rich ice—for example, at the surface of a comet or an icy planet or satellite—is expected to receive a non-negligible dose of high-energy photons, contributing to its partial photo-destruction and/or photochemical alteration. However, the fact that pyrimidine is shielded by a thick layer of ices and minerals in the ISM and the Solar System will allow it to survive longer times to harsh radiation, as supported by the detection of pyrimidine derivatives and other *N*-heterocycles in meteorites (Hayatsu, 1964, 1975; Folsome *et al.*, 1971, 1973; van der Velden and Schwartz, 1977; Stoks and Schwartz, 1979, 1981; Callahan *et al.*, 2011).

3.1.2. Formation of photo-products. The photo-destruction of pyrimidine is further witnessed by the emergence of new bands in the IR spectra recorded during irradiation, most of them corresponding to products formed after rupture of the pyrimidine ring (Fig. 3). A few examples of these are bands appearing at about 2340, 2262, 2168, 2136, 2085, and 1320 cm⁻¹ in the IR spectra of the ices irradiated with the 0th order light and the He II line (Fig. 3a and 3c, respectively). These peaks are assigned to CO₂ (Sandford and Allamandola, 1990), HNCO (Moore and Hudson, 2003), OCN⁻ (Schutte and Greenberg, 1997; Demyk *et al.*, 1998; Bernstein *et al.*, 2000), CO (Sandford *et al.*, 1988), CN⁻ (overlapping with CO in most cases; Moore and Hudson, 2003; Gerakines *et al.*, 2004), and HCOO⁻ (van Broekhuizen *et al.*, 2004), respectively. Since pyrimidine is the only source of carbon in our ice mixtures, these species can only be formed from the fragmentation of pyrimidine and

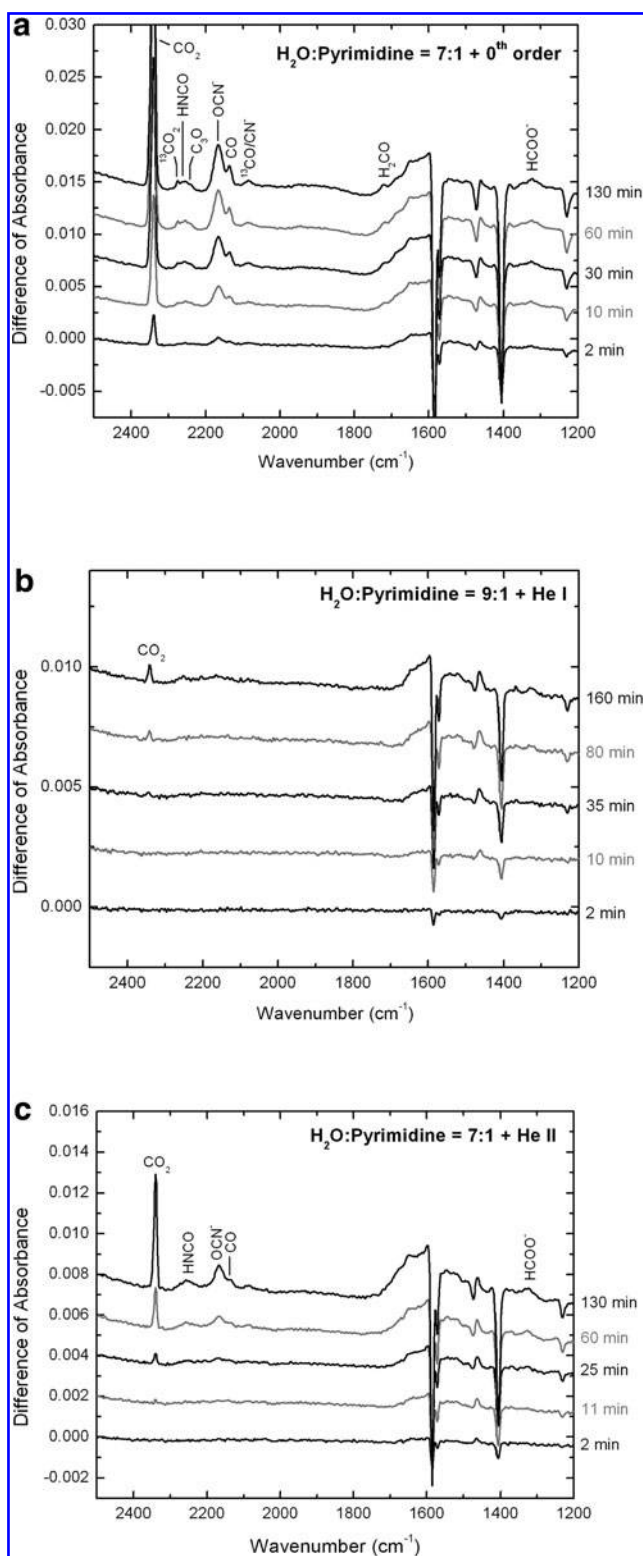


FIG. 3. Infrared spectra ($4000\text{--}850\text{ cm}^{-1}$) showing the differences of absorbance (relative to the spectra before irradiation) for the three H₂O:pyrimidine ice samples (1000 ML) irradiated with (a) the 0th order beam light for 2, 10, 30, 60, and 130 min; (b) the He I line for 2, 10, 35, 80, and 160 min; and (c) the He II line for 2, 11, 25, 60, and 130 min. The identified photo-products are indicated on the spectra according to the positions of their respective bands.

subsequent oxidation of these fragments. These peaks appear to be more intense in the case of the 0th order light sample compared to those for the He II line sample, which suggests again a more efficient photo-destruction of pyrimidine when the broad-range 4.1–49.6 eV beam is employed, and are in agreement with the half-lives (Eq. 1) and characteristic times (Eq. 2) derived for pyrimidine in those experiments (Tables 2 and 3).

The IR spectrum of the 0th order light ice also shows additional peaks near 2240 cm^{-1} , which can be assigned to C₃O (Gerakines *et al.*, 1996) or the CN radical (Wu *et al.*, 2012), and near 1720 cm^{-1} , assigned to H₂CO (Gerakines *et al.*, 1996), as well as weak peaks corresponding to ¹³CO₂ and ¹³CO at about 2275 and 2087 cm^{-1} , respectively (Fig. 3a).

In contrast, the IR spectra of the ice irradiated with the He I line only shows a weak band for CO₂ (Fig. 3b), which indicates a less efficient photo-destruction of pyrimidine when this light source is employed. This result is consistent with the longer photo-destruction half-life of pyrimidine in the corresponding irradiation experiment (Table 2).

Finally, a few minor bands, sometimes barely rising above the noise level, could be seen around 2135 (overlapping with CO), 1650 , 1515 , 1335 , 1110 , 1040 , and/or 1020 cm^{-1} in all three IR spectra (Fig. 3). These bands may be due to the presence of other species formed from fragments of pyrimidine, such as CH₂CHNC, CH₃CH=NH, NH₃⁺, C₂H₃CN⁺, CH₃CH=NH, H₂CNO, and C₂H₅CN (Shimanouchi, 1972; Stolkin *et al.*, 1977; Hashiguchi *et al.*, 1984; Delwiche *et al.*, 1993; McCluskey and Frei, 1993; Thompson and Jacox, 2001; Hudson and Moore, 2004; Danger *et al.*, 2011).

During these short irradiations of 1000 ML of H₂O:pyrimidine ices, the amount of pyrimidine was continuously decreasing either because of its photo-destruction or its photo-conversion into other products. This was, however, not the case for the long experiments, during which H₂O:pyrimidine mixtures were continuously deposited on the CaF₂ substrate, which increased the amounts of photo-products formed in the residues, both from the destruction and conversion of pyrimidine, including pyrimidine derivatives that cannot be detected with IR spectroscopy because of their small abundances. Their presence in our residues was therefore sought with the use of HPLC and GC-MS techniques.

3.2. Composition of the residues (HPLC/GC-MS)

High-performance liquid chromatography and gas chromatography coupled with mass spectrometry analyses provided independent, complementary information about the chemical composition of the residues recovered at room temperature after their UV/EUV irradiation at 14 K. Since this study was focused on the formation of uracil and its precursor 4(3H)-pyrimidone, we mainly searched for the presence of singly and doubly oxidized compounds in the residues and derived the abundances of 4(3H)-pyrimidone and uracil from the HPLC data in order to estimate their production yields.

3.2.1. HPLC analysis. Figure 4 shows the HPLC chromatograms ($\lambda=256\text{ nm}$ channel) of the three residues produced from the irradiation of H₂O:pyrimidine ice mixtures

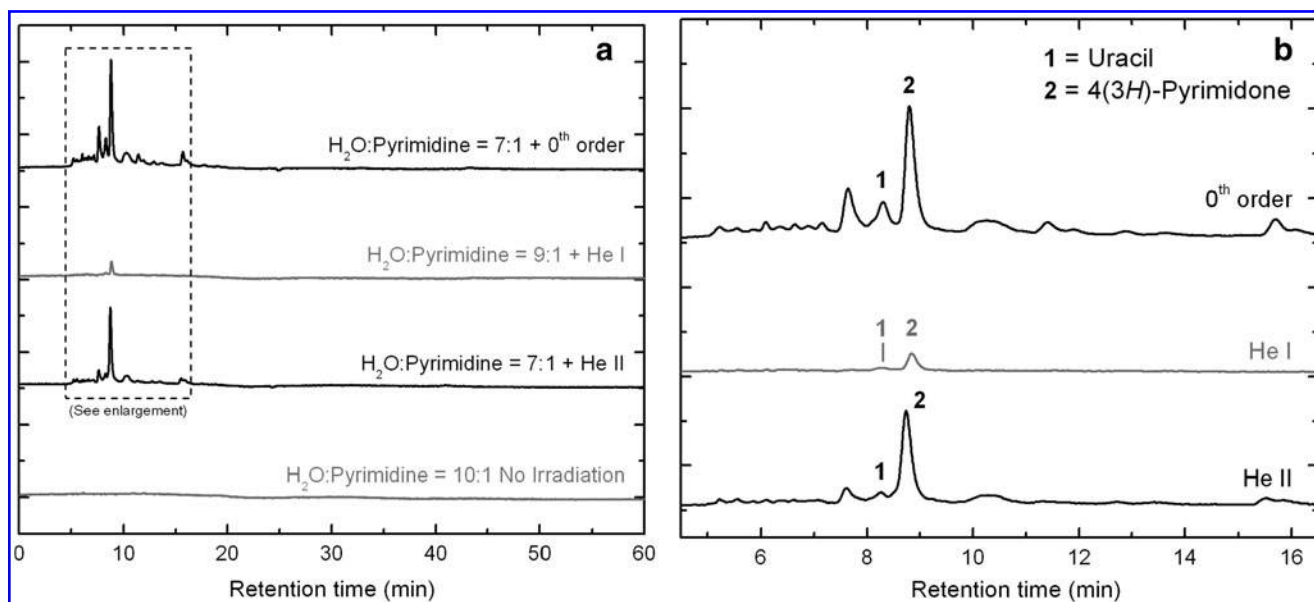


FIG. 4. (a) HPLC chromatograms ($\lambda=256$ nm) of the three residues produced from the UV/EUV irradiations of H_2O :pyrimidine ice mixtures with the 0^{th} order beam light (top trace, irradiation time: 20 h), the He I line (top middle trace, 32 h), and the He II line (bottom middle trace, 32 h). The bottom trace corresponds to an H_2O :pyrimidine = 10:1 ice mixture deposited on the substrate for 25 h but not photo-irradiated. (b) Enlargement of the chromatograms for the three residues to the range in which most peaks are eluting. The main identified photo-products are uracil (1) and 4(3H)-pyrimidone (2).

with the 0^{th} order beam light, the He I line, and the He II line (top three traces), compared with the chromatogram of an H_2O :pyrimidine = 10:1 ice mixture that was deposited for 25 h under similar conditions to the three other samples but not photo-irradiated (blank, bottom trace). In contrast to the chromatogram of the blank sample, which shows no peaks at all, the chromatograms of the three residues produced from the UV/EUV irradiations of pyrimidine in H_2O ice show a number of peaks among which only a few could be identified.

The first result that can be mentioned is the absence of pyrimidine in the three irradiated samples (Fig. 4, top three traces). This could be explained by either or both of the following reasons: (i) pyrimidine was fully consumed via photo-destruction and/or photo-conversion into other products, similarly to what was observed for comparable ices irradiated with an H_2 -discharge UV lamp (Nuevo *et al.*, 2009), and (ii) the remaining, unirradiated pyrimidine sublimed away during the warm-up from 14 K to room temperature.

The chromatogram of the sample irradiated with the 0^{th} order light (top trace) has some resemblance to that of H_2O :pyrimidine ice mixtures irradiated with an H_2 -discharge lamp (Nuevo *et al.*, 2009), which supports an efficient photo-conversion of pyrimidine into other products. In particular, it shows a number of peaks in the short retention time range ($R_t \leq 16$ min, Fig. 4b), with the largest intensities among the chromatograms of the three irradiated samples. The peaks for 4(3H)-pyrimidone ($R_t=8.78$ min) and uracil (8.30 min) could be easily identified by comparison of their retention times and UV spectra with the corresponding standards. Other peaks in this chromatogram could not be identified, either because of the weak signal to noise of their UV spectra or because of the lack of commercial standards.

The HPLC chromatogram of the residue produced from the irradiation of an H_2O :pyrimidine = 7:1 ice mixture with

the He II line (Fig. 4a, bottom middle trace) looks similar to that of the residue produced with the 0^{th} order light (top trace), with smaller intensities. 4(3H)-Pyrimidone (8.73 min) and uracil (8.25 min) could be clearly identified in this chromatogram, with different relative proportions compared with the 0^{th} order light residue. Finally, the chromatogram of the residue produced from an H_2O :pyrimidine = 9:1 ice mixture with the He I line (Fig. 4a, top middle trace) shows very few weak peaks. The peak at 8.84 min, assigned to 4(3H)-pyrimidone, is the only obvious peak in the whole chromatogram. The peak assigned to uracil ($R_t=8.34$ min) is very weak and overlapping with other weak peaks, but could be separated from the others during data analysis.

3.2.2. GC-MS analysis. The GC-MS chromatograms of the same three samples (Figs. 5 and 6) confirm the presence of 4(3H)-pyrimidone and uracil in all of them by comparison of both their retention times and mass spectra (Fig. 6). Comparison of the chromatograms of the residues with those of the unirradiated sample (Fig. 5, bottom middle trace) and of the agent (MTBSTFA) which was used to derivatize all samples and all standards (bottom trace), indicates that only a few peaks in the residue chromatograms are due to the presence of photo-products formed from the UV/EUV irradiation of the starting H_2O :pyrimidine ices.

Data from the GC-MS single-ion chromatograms (SICs) of the residues could also show the presence of a few other products, including 2,2'-bipyrimidine (158 amu) and urea (231 amu) in all three samples, as well as small quantities of 2-hydroxypyrimidine (153 amu) and 4,6-dihydroxypyrimidine (283 amu) in the samples formed from the irradiations with the 0^{th} order light and the He II line. All these compounds were previously observed in residues formed from the UV irradiation of H_2O :pyrimidine ice mixtures with an H_2 -discharge lamp (Nuevo *et al.*, 2009). The

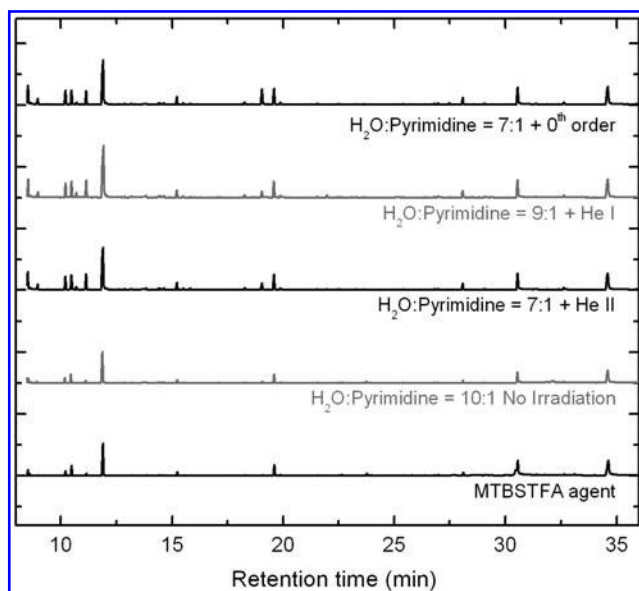


FIG. 5. GC-MS total-ion chromatograms (TICs) of the three residues produced from the UV/EUV irradiations of H₂O:pyrimidine ice mixtures with the 0th order beam light (top trace, irradiation time: 20 h), the He I line (top middle trace, 32 h), and the He II line (middle trace, 32 h). The bottom middle trace corresponds to the TIC of the same H₂O:pyrimidine=10:1 ice mixture deposited on the substrate for 25 h but not photo-irradiated, whose HPLC chromatogram is shown in Fig. 4a. The bottom trace corresponds to the injection of the MTBSTFA agent used to derivatize all residues, control samples, and standards in this study.

detection of 2,2'-bipyrimidine, which consists of two molecules of pyrimidine bound via a C–C bond, indicates that UV/EUV can excite and/or ionize pyrimidine to make it reactive and react with another pyrimidine molecule, while that of urea (NH₂CONH₂) in measurable quantities supports the photo-induced rupture of the pyrimidine ring and the subsequent photo-oxidation of the resulting fragments inferred from the IR spectroscopy data (see Section 3.1).

4. Discussion

4.1. Production of 4(3H)-pyrimidone and uracil

For each HPLC chromatogram of the three samples irradiated with the UV/EUV sources, the peaks assigned to 4(3H)-pyrimidone and uracil were analyzed with the Fityk software in order to separate multiple overlapping peaks. Once these peaks were separated, their areas could be derived; and by comparison with the chromatograms of the corresponding standards, the total quantities of 4(3H)-pyrimidone and uracil in each residue could be estimated.

As absolute quantities can vary from one sample to another, even for residues produced from the same starting ice mixture irradiated with the same UV/EUV light, we used these quantities to estimate the molecular production yields for 4(3H)-pyrimidone and uracil, which are defined here as the numbers of molecules of pyrimidine needed to form one molecule of 4(3H)-pyrimidone or uracil. These molecular yields, summarized in Table 4, were obtained after accounting for the fact that only 10–15% of the pyrimidine deposited on the CaF₂ substrate were actually exposed to UV/EUV radiation because of the small synchrotron beam

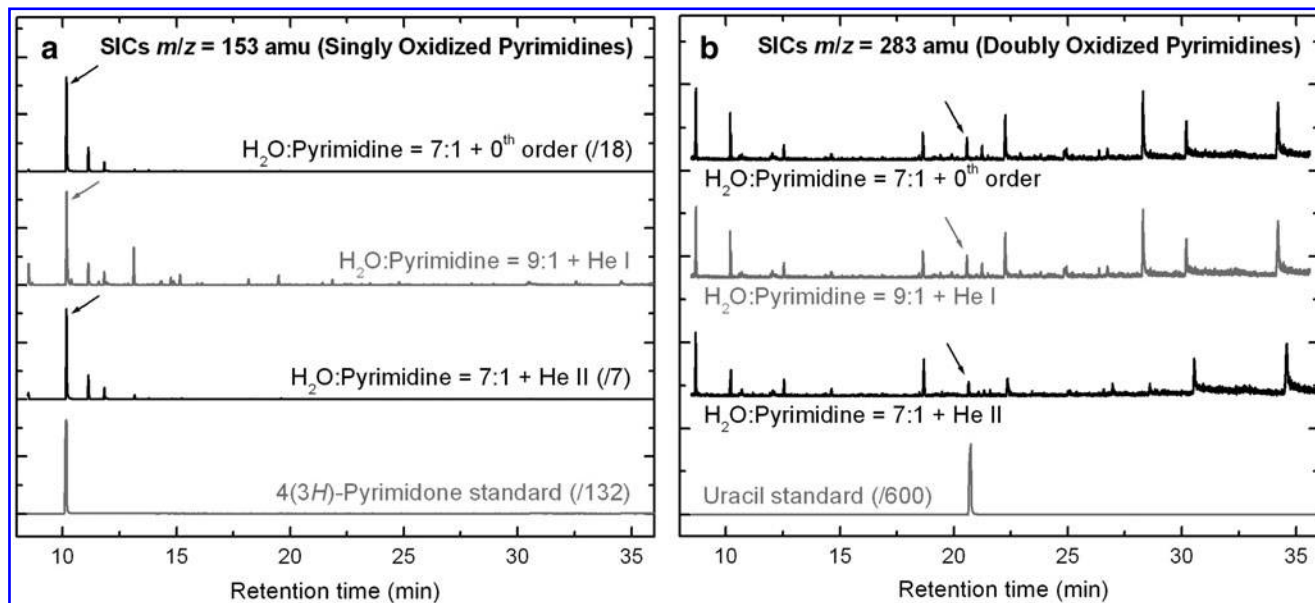


FIG. 6. (a) GC-MS single-ion chromatograms (SICs) of the three residues produced from the UV/EUV irradiations of H₂O:pyrimidine ice mixtures with the 0th order beam light (top trace, irradiation time: 20 h), the He I line (top middle trace, 32 h), and the He II line (bottom middle trace, 32 h), for $m/z = 153$ amu, which corresponds to the mass of singly oxidized pyrimidine derivatives. The bottom trace is the SIC of a 4(3H)-pyrimidone standard prepared and injected under the same conditions as the residues. (b) GC-MS SICs of the same three residues for $m/z = 283$ amu, which corresponds to the mass of doubly oxidized pyrimidine derivatives. The bottom trace is the SIC of a uracil standard prepared and injected under the same conditions as the residues. Identifications of 4(3H)-pyrimidone and uracil in the residues are marked with arrows.

TABLE 4. MOLECULAR PRODUCTION YIELDS (NUMBER OF MOLECULES OF PYRIMIDINE DEPOSITED NEEDED TO PRODUCE ONE MOLECULE OF A GIVEN PRODUCT) AND RELATIVE PROPORTIONS (RATIOS) ESTIMATED FOR 4(3H)-PYRIMIDONE AND URACIL IN THE RESIDUES PRODUCED FROM THE UV/EUV IRRADIATION OF H₂O:PYRIMIDINE ICES WITH THE 0TH ORDER BEAM LIGHT, THE HE I LINE, AND THE HE II LINE

Sample	4(3H)-Pyrimidone	Uracil	Ratio
0 th order light	1/450	1/1900	4.4
He I line	1/1.4 × 10 ⁴	1/3.6 × 10 ⁶	254
He II line	1/3400	1/1.2 × 10 ⁵	36.5
H ₂ lamp	1/670	1/9300	13.9

Values are compared with what was obtained for a residue produced from an H₂O:pyrimidine = 20:1 ice mixture photo-irradiated with an H₂-discharge lamp (Nuevo *et al.*, 2009).

size compared with the deposition area on the substrate. In addition, these molecular production yields were normalized to account for the differences between the irradiation times (20 h for the 0th order light, and 32 h for the He I and He II lines) and the wavelength ranges of the beams in each experiment (about 275 nm for the 0th order light beam and 0.2 nm for the He I and He II lines). The irradiation time and wavelength range used for the H₂-discharge lamp experiment were 23 h and 70 nm, respectively (Nuevo *et al.*, 2009).

As suggested by previous experimental and theoretical studies, 4(3H)-pyrimidone is mostly formed from the photo-oxidation of pyrimidine, while uracil is formed from the photo-oxidation of two possible singly oxidized derivatives of pyrimidine, among which 4(3H)-pyrimidone is the most abundant and stable isomer and, therefore, the most probable precursor of uracil in irradiation experiments (Nuevo *et al.*, 2009; Bera *et al.*, 2010). Consequently, the production yield of 4(3H)-pyrimidone is directly related to the photo-oxidation efficiency of pyrimidine, while that of uracil is strongly correlated with the photo-oxidation efficiency of 4(3H)-pyrimidone.

Nonetheless, production yields should not be seen merely as the efficiency of forming a compound from its precursor but rather as the net result of the competition between a set of photo-induced reactions leading to the formation of more complex molecules and an independent set of photo-induced reactions leading to the destruction of the starting compounds and newly formed photo-products. In addition, it must be noted that the photo-induced reactions that take place in the experiments described in the present study may be the consequence of the absorption of a UV/EUV photon not only by pyrimidine and its derivatives but also by H₂O, even though the following discussion will only focus on the production of pyrimidine-based compounds.

Molecular yields show that the 0th order light is more efficient for producing both 4(3H)-pyrimidone and uracil than any other light source employed (Table 4). The second most efficient light source for producing those two photo-products is the H₂-discharge lamp, while the molecular yields obtained for 4(3H)-pyrimidone and uracil with the monochromatic sources (He I and He II lines) are significantly smaller than those obtained for the broad

energy sources (0th order light and H₂-discharge lamp). The He I line was found to be the least efficient light source among all those studied here, with production yields for 4(3H)-pyrimidone and uracil about 8 and 65 times smaller than those derived for the 0th order light experiment, respectively, and about 4 and 29 times smaller than those derived for the He II line experiment, respectively (Table 4). Such a result was expected from the very small number of peaks seen in the HPLC chromatogram of this residue (Fig. 4) and from the longer photo-destruction half-life derived for pyrimidine in this experiment (Table 2). It also shows that the absorption of higher-energy photons emitted by a monochromatic light source (He II, 40.8 eV) results in higher production yields than when a monochromatic source with lower-energy photons is employed (He I, 21.2 eV).

The other interesting parameter to be compared between the samples is the relative abundances—or molecular yield—of 4(3H)-pyrimidone and uracil. These ratios, given in the last column of Table 4, were obtained by dividing the abundance—or molecular yield—of 4(3H)-pyrimidone by that of uracil in each residue. The 4(3H)-pyrimidone to uracil ratio in the sample irradiated with the 0th order light (4.4) is about 3 times smaller than that measured for the sample irradiated with the H₂-discharge lamp (13.9) (Nuevo *et al.*, 2009), which indicates that the production of uracil from its precursors is more efficient when the 0th order beam is employed. This difference is most probably due to the fact that the energy range of the 0th order light beam is broader (about 4 times) than that of the H₂-discharge lamp. Indeed, the broader the UV/EUV range, the higher the probability for a photon with the right energy to be absorbed by the newly formed photo-produced pyrimidine derivatives, including 4(3H)-pyrimidone and its isomers—in their neutral, cationic, and/or radical forms—and thus the higher the probability for those species to be converted into more complex products, including uracil and its isomers.

In contrast, photons emitted by monochromatic light sources such as the He I and He II lines will have a significantly smaller probability to be absorbed by the potential precursors of uracil and its isomers, resulting in smaller conversion rates and final production yields. However, as mentioned earlier, increasing the probability of absorbing photons does not necessarily result in an increase of the production of more complex molecules, since photons of given energies can also selectively destroy specific chemical bonds and lead to the photo-destruction or fragmentation of both the starting and the newly formed species. Nonetheless, the results summarized in Table 4 clearly indicate that the combinations of those photo-induced production and destruction processes in the experiments described in the present study always result in the production of more complex molecules, whose yields are correlated with the energy range of the incident light source.

4.2. Astrobiological implications

Studying the photo-formation and photo-stability of molecules such as pyrimidine and derivatives including nucleobases is important from an astrobiological point of view because such compounds have been detected in meteorites, together with a number of other purine-based

nucleobases such as adenine, guanine, xanthine, and hypoxanthine (Hayatsu, 1964, 1975; Folsome *et al.*, 1971, 1973; van der Velden and Schwartz, 1977; Stoks and Schwartz, 1979, 1981; Callahan *et al.*, 2011). In particular, the reported detections of 4(3*H*)-pyrimidone (sometimes named 4-hydroxy-pyrimidine) and uracil in the carbonaceous chondrites Murchison, Murray, and Orgueil (Folsome *et al.*, 1971, 1973; Lawless *et al.*, 1972; Stoks and Schwartz, 1979) suggest that these compounds can survive ionizing radiation from the astrophysical environment where they formed to the formation of the Solar System and their delivery to telluric planets via comets and asteroids.

The results obtained from our experiments are in agreement with such a scenario, as they demonstrated that the irradiation of simple H₂O:pyrimidine ice mixtures with high-energy UV/EUV sources always leads to the formation of complex molecules including the nucleobase uracil. Although the three light sources employed in our experiments have different effects on the photo-destruction of pyrimidine, the formation of photo-products, and the photo-stability of the newly formed products to the incident photo-irradiation (Section 3), the photo-destruction half-lives derived for pyrimidine indicate that, when embedded in an H₂O ice matrix, pyrimidine may survive for long periods of time in astrophysical environments.

In these environments, ice compositions are far more complex, as they usually consist of mixtures of H₂O (dominant component) as well as CH₃OH, CO, CO₂, CH₄, and NH₃ (Gibb *et al.*, 2000, 2004; Dartois, 2005). Therefore, if pyrimidine and its products of photo-irradiation, including 4(3*H*)-pyrimidone and uracil, are shielded from harsh UV/EUV radiation by such complex ices, nucleobases as well as a host of other molecules of prebiotic interest including amino acids and sugars (Kvenvolden *et al.*, 1970; Cronin and Pizzarello, 1999; Cooper *et al.*, 2001; Sephton, 2002) may have formed abiotically, survived throughout the formation of the Solar System, and seeded the early Earth during the heavy meteoritic bombardment (Chyba and Sagan, 1992). This primordial prebiotic soup on Earth (Oró, 1961) may have subsequently triggered the first biological reactions that led to the emergence of life on our planet about 3.8 billion years ago.

5. Conclusions

This experimental study shows that the irradiation of pyrimidine in pure H₂O ice at low temperature with several UV/EUV light sources (0th order beam light, He I line, and He II line) always leads to the formation of the nucleobase uracil and its precursor 4(3*H*)-pyrimidone. These two compounds were detected in the residues obtained after warming the samples to room temperature. However, the energy and the energy range of the incident photon sources had significantly different effects on both the photo-destruction of pyrimidine and its conversion into photo-products, as well as on the photo-stability of these newly formed photo-products such as uracil and its precursor 4(3*H*)-pyrimidone. In particular, our results show that the energy range of the light source employed is correlated with the production yields of 4(3*H*)-pyrimidone and uracil.

In all cases, our study indicates that pyrimidine and its derivatives, including nucleobases, can survive the high-

energy UV/EUV irradiation field present during and after the formation of the Solar System if embedded in—and shielded by—an H₂O-rich ice matrix, as is the case in cold, primitive astrophysical objects such as comets. The detection of pyrimidine-based compounds in meteorites strongly supports our results and a scenario in which organic molecules of prebiotic interest such as nucleobases were formed in astrophysical environments before they were delivered to the early Earth, eventually leading to the emergence of life.

Acknowledgments

This work was supported by the NSC grants #99-2112-M-008-011-MY3 and #101-2811-M-008-023 (T.-S.Y.), the National Synchrotron Radiation Research Center, and the NSF Planetary Astronomy Program under grant AST-1108898 (C.-Y.R.W.). M.N. acknowledges S.A. Sandford for the use of the HPLC and GC-MS devices at the Astrophysics & Astrochemistry Laboratory of NASA Ames Research Center. The authors are grateful for the helpful reviews of two anonymous reviewers, from which this manuscript benefited significantly.

Author Disclosure Statement

No competing financial interests exist.

Abbreviations

EUV, extreme ultraviolet; GC-MS, gas chromatography coupled with mass spectrometry; HPLC, high-performance liquid chromatography; ISM, interstellar medium; ML, monolayers; MTBSTFA, *N*-(*tert*-butyldimethylsilyl)-*N*-methyltrifluoroacetamide; PAHs, polycyclic aromatic hydrocarbons; PANHs, polycyclic aromatic nitrogen heterocycles; SICs, single-ion chromatograms; TICs, total-ion chromatograms; UHV, ultrahigh vacuum.

References

- Allamandola, L.J., Tielens, A.G.G.M., and Barker, J.R. (1989) Interstellar polycyclic aromatic hydrocarbons—the infrared emission bands, the excitation/emission mechanism, and the astrophysical implications. *Astrophys J Suppl Ser* 71:733–775.
- Barr, J.D., De Fanis, A., Dyke, J.M., Gamblin, S.D., Hooper, N., Morris, A., Stranges, S., West, J.B., and Wright, T.G. (1999) Study of the OH and OD radicals with photoelectron spectroscopy using synchrotron radiation. *J Chem Phys* 110:345–354.
- Bera, P.P., Nuevo, M., Milam, S.N., Sandford, S.A., and Lee, T.J. (2010) Mechanism for the abiotic synthesis of uracil via UV-induced oxidation of pyrimidine in pure H₂O ices under astrophysical conditions. *J Chem Phys* 133:104303 (7pp).
- Bernstein, M.P., Sandford, S.A., and Allamandola, L.J. (2000) H, C, N, and O isotopic substitution studies of the 2165 cm⁻¹ (4.62 μm) “XCN” feature produced by UV photolysis of mixed molecular ices. *Astrophys J* 542:894–897.
- Bernstein, M.P., Sandford, S.A., and Allamandola, L.J. (2005) The mid-infrared absorption spectra of neutral polycyclic aromatic hydrocarbons in conditions relevant to dense interstellar clouds. *Astrophys J Suppl Ser* 161:53–64.
- Brünken, S., McCarthy, M.C., Thaddeus, P., Godfrey, P.D., and Brown, R.D. (2006) Improved line frequencies for the nucleic acid base uracil for a radioastronomical search. *Astron Astrophys* 459:317–320.

- Callahan, M.P., Smith, K.E., Cleaves, H.J., II, Ruzicka, J., Stern, J.C., Glavin, D.P., House, C.H., and Dworkin, J.P. (2011) Carbonaceous meteorites contain a wide range of extraterrestrial nucleobases. *Proc Natl Acad Sci USA* 108:13995–13998.
- Casal, S., Mendes, E., Fernandes, J.O., Oliveira, M.B.P.P., and Ferreira, M.A. (2004) Analysis of heterocyclic aromatic amines in foods by gas chromatography–mass spectrometry as their *tert*-butyldimethylsilyl derivatives. *J Chromatogr A* 1040:105–114.
- Charnley, S.B., Kuan, Y.-J., Huang, H.-C., Botta, O., Butner, H.M., Cox, N., Despois, D., Ehrenfreund, P., Kisiel, Z., Lee, Y.-Y., Markwick, A.J., Peeters, Z., and Rodgers, S.D. (2005) Astronomical searches for nitrogen heterocycles. *Adv Space Res* 36:137–145.
- Chen, Y.-J., Chuang, K.-Y., Muñoz Caro, G.M., Nuevo, M., Chu, C.-C., Yih, T.-S., Ip, W.-H., and Wu, C.-Y.R. (2014) Vacuum ultraviolet emission spectrum measurement of a microwave-discharge hydrogen-flow lamp in several configurations: application to photodesorption of CO ice. *Astrophys J* 781:15 (13pp).
- Chyba, C.F. and Sagan, C. (1992) Endogenous production, exogenous delivery and impact-shock synthesis of organic molecules: an inventory for the origins of life. *Nature* 335: 125–132.
- Cooper, G., Kimmich, N., Belisle, W., Sarinana, J., Brabham, K., and Garrel, L. (2001) Carbonaceous meteorites as a source of sugar-related organic compounds for the early Earth. *Nature* 414:879–883.
- Cronin, J.R. and Pizzarello, S. (1999) Amino acid enantiomer excesses in meteorites: origin and significance. *Adv Space Res* 23:293–299.
- Danger, G., Bossa, J.-B., de Marcellus, P., Borget, F., Duvernay, F., Theulé, P., Chiavassa, T., and d’Hendecourt, L. (2011) Experimental investigation of nitrile formation from VUV photochemistry of interstellar ices analogs: acetonitrile and amino acetonitrile. *Astron Astrophys* 525:A30 (6pp).
- Dartois, E. (2005) The ice survey opportunity of ISO. *Space Sci Rev* 119:293–310.
- Delwiche, J., Gochel-Dupuis, M., Collin, J.E., and Heinesch, J. (1993) High resolution HeI photoelectron spectrum of acrylonitrile. *J Electron Spectrosc Relat Phenomena* 66:65–74.
- Demyk, K., Dartois, E., d’Hendecourt, L., Jourdain de Muizon, M., Heras, A.M., and Breiffellner, M. (1998) Laboratory identification of the 4.62 μm solid state absorption band in the ISO-SWS spectrum of RAFGL 7009S. *Astron Astrophys* 339:553–560.
- Folsome, C.E., Lawless, J., Romiez, M., and Ponnampereuma, C. (1971) Heterocyclic compounds indigenous to the Murchison meteorite. *Nature* 232:108–109.
- Folsome, C.E., Lawless, J., Romiez, M., and Ponnampereuma, C. (1973) Heterocyclic compounds recovered from carbonaceous chondrites. *Geochim Cosmochim Acta* 37:455–465.
- Frenklach, M. and Feigelson, E.D. (1989) Formation of polycyclic aromatic hydrocarbons in circumstellar envelopes. *Astrophys J* 341:372–384.
- Gerakines, P.A., Schutte, W.A., and Ehrenfreund, P. (1996) Ultraviolet processing of interstellar ice analogs. I. Pure ices. *Astron Astrophys* 312:289–305.
- Gerakines, P.A., Moore, M.H., and Hudson, R.L. (2004) Ultraviolet photolysis and proton irradiation of astrophysical ice analogs containing hydrogen cyanide. *Icarus* 170:202–213.
- Gibb, E.L., Whittet, D.C.B., Schutte, W.A., Boogert, A.C.A., Chiar, J.E., Ehrenfreund, P., Gerakines, P.A., Keane, J.V., Tielens, A.G.G.M., van Dishoeck, E.F., and Kerkhof, O. (2000) An inventory of interstellar ices toward the embedded protostar W33A. *Astrophys J* 536:347–356.
- Gibb, E.L., Whittet, D.C.B., Boogert, A.C.A., and Tielens, A.G.G.M. (2004) Interstellar ice: the Infrared Space Observatory legacy. *Astrophys J Suppl Ser* 151:35–73.
- Hashiguchi, K., Hamada, Y., Tsuboi, M., Koga, Y., and Kondo, S. (1984) Pyrolysis of amines: infrared spectrum of ethyldeneimine. *J Mol Spectrosc* 105:81–92.
- Hayatsu, R. (1964) Orgueil meteorite: organic nitrogen contents. *Science* 146:1291–1293.
- Hayatsu, R., Anders, E., Studier, M.H., and Moore, L.P. (1975) Purines and triazines in the Murchison meteorite. *Geochim Cosmochim Acta* 39:471–488.
- Hudgins, D.M., Sandford, S.A., Allamandola, L.J., and Tielens, A.G.G.M. (1993) Mid- and far-infrared spectroscopy of ices: optical constants and integrated absorbances. *Astrophys J Suppl Ser* 86:713–870.
- Hudson, R.L. and Moore, M.H. (2004) Reactions of nitriles in ices relevant to Titan, comets, and the interstellar medium: formation of cyanate ion, ketenimines, and isonitriles. *Icarus* 172:466–478.
- Itikawa, Y., Ichimura, K., Onda, K., Sakimoto, K., Takayanagi, K., Hatano, Y., Hayashi, M., Nishimura, H., and Tsurubuchi, S. (1989) Cross sections for collisions of electrons and photons with oxygen molecules. *Journal of Physical and Chemical Reference Data* 18:23–42.
- Judge, P.G. and Pietarila, A. (2004) On the formation of extreme-ultraviolet helium lines in the Sun: analysis of SOHO data. *Astrophys J* 606:1258–1275.
- Kobayashi, K. and Tsuji, T. (1997) Abiotic synthesis of uracil from carbon monoxide, nitrogen and water by proton irradiation. *Chem Lett* 1997:903–904.
- Kuan, Y.-J., Yan, C.-H., Charnley, S.B., Kisiel, Z., Ehrenfreund, P., and Huang, H.-C. (2003) A search for interstellar pyrimidine. *Mon Not R Astron Soc* 345:650–656.
- Kuan, Y.-J., Charnley, S.B., Huang, H.-C., Kisiel, Z., Ehrenfreund, P., Tseng, W.-L., and Yan, C.-H. (2004) Searches for interstellar molecules of potential prebiotic importance. *Adv Space Res* 33:31–39.
- Kvenvolden, K., Lawless, J., Pering, K., Peterson, E., Flores, J., and Ponnampereuma, C. (1970) Evidence for extraterrestrial amino-acids and hydrocarbons in the Murchison meteorite. *Nature* 228:923–926.
- Lawless, J.G., Folsome, C.E., and Kvenvolden, K.A. (1972) Organic matter in meteorites. *Sci Am* 226:38–46.
- MacKenzie, S.L., Tenaschuk, D., and Fortier, G. (1987) Analysis of amino acids by gas-liquid chromatography as *tert*-butyldimethylsilyl derivatives: preparation of derivatives in a single reaction. *J Chromatogr* 387:241–253.
- Martins, Z., Botta, O., Fogel, M.L., Sephton, M.A., Glavin, D.P., Watson, J.S., Dworkin, J.P., Schwartz, A.W., and Ehrenfreund, P. (2008) Extraterrestrial nucleobases in the Murchison meteorite. *Earth Planet Sci Lett* 270:130–136.
- Materese, C.K., Nuevo, M., Bera, P.P., Lee, T.J., and Sandford, S.A. (2013) Thymine and other prebiotic molecules produced from the ultraviolet photo-irradiation of pyrimidine in simple astrophysical ice analogs. *Astrobiology* 13:948–962.
- McCluskey, M. and Frei, H. (1993) Transfer of methylene from ketene to nitric oxide by photoexcitation of reactant pairs in solid argon below the CH₂:C:O dissociation limit. *J Phys Chem* 97:5204–5207.
- Meier, R.R. (1991) Ultraviolet spectroscopy and remote sensing of the upper atmosphere. *Space Sci Rev* 58:1–185.

- Mendoza, E., Almeida, G.C., Andrade, D.P.P., Luna, H., Wolff, W., Rocco, M.L.M., and Boechat-Roberty, H.M. (2013) X-ray photodesorption and proton destruction in protoplanetary discs: pyrimidine. *Mon Not R Astron Soc* 433:3440–3452.
- Miyakawa, S., Yamanashi, H., Kobayashi, K., Cleaves, H.J., and Miller, S.L. (2002) Prebiotic synthesis from CO atmosphere: implications for the origins of life. *Proc Natl Acad Sci USA* 99:14628–14631.
- Moore, M.H. and Hudson, R.L. (2003) Infrared study of ion-irradiated N₂-dominated ices relevant to Triton and Pluto: formation of HCN and HNC. *Icarus* 161:486–500.
- Nuevo, M., Milam, S.N., Sandford, S.A., Elsila, J.E., and Dworkin, J.P. (2009) Formation of uracil from the ultraviolet photo-irradiation of pyrimidine in pure H₂O ices. *Astrobiology* 9:683–695.
- Nuevo, M., Milam, S.N., and Sandford, S.A. (2012) Nucleobases and prebiotic molecules in organic residues produced from the ultraviolet photo-irradiation of pyrimidine in NH₃ and H₂O+NH₃ ices. *Astrobiology* 12:295–314.
- Öberg, K.I., Fuchs, G.W., Awad, Z., Fraser, H.J., Schlemmer, S., van Dishoeck, E.F., and Linnartz, H. (2007) Photodesorption of CO ice. *Astrophys J* 662:L23–L26.
- Öberg, K.I., van Dishoeck, E.F., and Linnartz, H. (2009) Photodesorption of ices I: CO, N₂, and CO₂. *Astron Astrophys* 496:281–293.
- Oró, J. (1961) Comets and the formation of biochemical compounds on the primitive Earth. *Nature* 190:389–390.
- Peeters, Z., Botta, O., Charnley, S.B., Kisiel, Z., Kuan, Y.-J., and Ehrenfreund, P. (2005) Formation and photostability of N-heterocycles in space. I. The effect of nitrogen on the photostability of small aromatic molecules. *Astron Astrophys* 433:583–590.
- Peter, H., Gudiksen, B.V., and Nordlund, Å. (2006) Forward modeling of the corona of the Sun and solar-like stars: from a three-dimensional magnetohydrodynamic model to synthetic extreme-ultraviolet spectra. *Astrophys J* 638:1086–1100.
- Pilling, S., Andrade, D.P.P., do Nascimento, E.M., Marinho, R.R.T., Boechat-Roberty, H.M., de Coutinho, L.H., de Souza, G.G.B., de Castilho, R.B., Cavasso-Filho, R.L., Lago, A.F., and de Brito, A.N. (2011) Photostability of gas- and solid-phase biomolecules within dense molecular clouds due to soft X-rays. *Mon Not R Astron Soc* 411:2214–2222.
- Puget, J.L. and Léger, A. (1989) A new component of the interstellar matter—small grains and large aromatic molecules. *Annu Rev Astron Astrophys* 27:161–198.
- Rees, M.H. (1989) *Physics and Chemistry of the Upper Atmosphere*, Cambridge University Press, Cambridge, UK, pp 8–11.
- Ricca, A., Bauschlicher, C.W., and Bakes, E.L.O. (2001) A computational study of the mechanisms for the incorporation of a nitrogen atom into polycyclic aromatic hydrocarbons in the Titan haze. *Icarus* 154:516–521.
- Roelfsema, P.R., Cox, P., Tielens, A.G.G.M., Allamandola, L.J., Baluteau, J.P., Barlow, M.J., Beintema, D., Boxhoorn, D.R., Cassinelli, J.P., Caux, E., Churchwell, E., Clegg, P.E., de Graauw, T., Heras, A.M., Huygen, R., van der Hucht, K.A., Hudgins, D.M., Kessler, M.F., Lim, T., and Sandford, S.A. (1996) SWS observations of IR emission features towards compact HII regions. *Astron Astrophys* 315:L289–L292.
- Ruscic, B., Wagner, A.F., Harding, L.B., Asher, R.L., Feller, D., Dixon, D.A., Peterson, K.A., Song, Y., Qian, X., Ng, C.-Y., Liu, J., Chen, W., and Schwenke, D.W. (2002) On the enthalpy of formation of hydroxyl radical and gas-phase bond dissociation energies of water and hydroxyl. *J Phys Chem A* 106:2727–2747.
- Sandford, S.A. and Allamandola, L.J. (1990) The physical and infrared spectral properties of CO₂ in astrophysical ice analogs. *Astrophys J* 355:357–372.
- Sandford, S.A., Allamandola, L.J., Tielens, A.G.G.M., and Valero, G. (1988) Laboratory studies of the infrared spectral properties of CO in astrophysical ices. *Astrophys J* 329:498–510.
- Sandford, S.A., Bernstein, M.P., and Allamandola, L.J. (2004) The mid-infrared laboratory spectra of naphthalene (C₁₀H₈) in solid H₂O. *Astrophys J* 607:346–360.
- Schummer, C., Delhomme, O., Appenzeller, B.M.R., Wenning, R., and Millet, M. (2009) Comparison of MTSBTFA and BSTFA in derivatization reactions of polar compounds prior to GC/MS analysis. *Talanta* 77:1473–1482.
- Schutte, W.A. and Greenberg, J.M. (1997) Further evidence for the OCN⁻ assignment to the XCN band in astrophysical ice analogs. *Astron Astrophys* 317:L43–L46.
- Sephton, M.A. (2002) Organic compounds in carbonaceous meteorites. *Nat Prod Rep* 19:292–311.
- Shimanouchi, T. (1972) *Tables of Molecular Vibrational Frequencies Consolidated*, Vol. I, National Bureau of Standards, U.S. Government Printing Office, Washington, DC.
- Simon, M.N. and Simon, M. (1973) Search for interstellar acrylonitrile, pyrimidine, and pyridine. *Astrophys J* 184:757–762.
- Stephens, J.A. and McKoy, V. (1987) Photoionization of the valence orbitals of OH. *J Chem Phys* 88:1737–1742.
- Stoks, P.G. and Schwartz, A.W. (1979) Uracil in carbonaceous meteorites. *Nature* 282:709–710.
- Stoks, P.G. and Schwartz, A.W. (1981) Nitrogen-heterocyclic compounds in meteorites: significance and mechanisms of formation. *Geochim Cosmochim Acta* 45:563–569.
- Stolkin, I., Ha, T.-K., and Günthard, H.S. (1977) N-methylmethyleneimine and ethylideneimine: gas- and matrix-infrared spectra, *ab initio* calculations and thermodynamic properties. *Chem Phys* 21:327–347.
- Thompson, W.E. and Jacox, M.E. (2001) The infrared spectra of the NH₃ – d_n⁺ cations trapped in solid neon. *J Chem Phys* 114:4846–4854.
- van Broekhuizen, F.A., Keane, J.V., and Schutte, W.A. (2004) A quantitative analysis of OCN⁻ formation in interstellar ice analogs. *Astron Astrophys* 415:425–436.
- van der Velden, W. and Schwartz, A.W. (1977) Search for purines and pyrimidines in the Murchison meteorite. *Geochim Cosmochim Acta* 41:961–968.
- Wu, C.-Y.R., Judge, D.L., Cheng, B.-M., Shih, W.-H., Yih, T.-S., and Ip, W.-H. (2002) Extreme ultraviolet photon-induced chemical reactions in the C₂H₂–H₂O mixed ices at 10 K. *Icarus* 156:456–473.
- Wu, Y.-J., Wu, C.-Y.R., Chou, S.-L., Lin, M.-Y., Lu, H.-C., Lo, J.-I., and Cheng, B.-M. (2012) Spectra and photolysis of pure nitrogen and methane dispersed in solid nitrogen with vacuum-ultraviolet light. *Astrophys J* 746:175 (11pp).
- Yamanashi, H., Takeda, S., Murasawa, K.-I., Miyakawa, S., Kaneko, T., and Kobayashi, K. (2001) Identification and determination of nucleic acid bases abiotically formed in simulated planetary atmospheres. *Anal Sci (Suppl)* 17:i1639–i1642.

Address correspondence to:
 Michel Nuevo
 NASA Ames Research Center
 Space Science Division
 MS 245-6
 Moffett Field, CA 94035
 E-mail: michel.nuevo-1@nasa.gov

Submitted 28 August 2013
 Accepted 14 January 2014